



# Modeling and desirability approach-based multi-response optimization of WEDM parameters in machining of aluminum metal matrix composite

Harmesh Kumar<sup>1</sup> · Alakesh Manna<sup>2</sup> · Rajesh Kumar<sup>3</sup>

Received: 7 July 2017 / Accepted: 16 August 2018 / Published online: 28 August 2018  
© The Brazilian Society of Mechanical Sciences and Engineering 2018

## Abstract

The study presents machining aspects of particulate silicon carbide reinforced aluminium metal matrix composite (Al/SiC<sub>p</sub>-MMC) using wire-cut electric discharge machining process. The influences of process parameters such as pulse on time, pulse off time, spark gap voltage, peak current, wire tension and wire feed rate on response variables such as workpiece cutting speed, surface roughness ( $R_a$ ) and spark gap have been investigated. The Box–Behnken's design has been utilized to plan the experiments, and response surface methodology is employed for developing quadratic regression models for selected response variables. Desirability function approach has been used to solve the multi-response optimization problem by assigning the weightages to the selected responses as per the user's requirement of quality or productivity. The study recommends optimal process conditions such as pulse on time 0.75  $\mu$ s, pulse off time 16  $\mu$ s, spark gap voltage 35 V, peak current 120 A, wire tension 1200 g, and wire feed rate 10 m/min for effective machining of Al/SiC<sub>p</sub>-MMC, which has been validated by conducting confirmation experiments. The developed regression models for selected responses revealed compatible results, thereby justifying their acceptability.

**Keywords** Metal matrix composites · Wire-cut electric discharge machining · Optimization · Response surface methodology · Scanning electron microscope · Box–Behnken's design

## Abbreviations

Al-MMCs Aluminum metal matrix composites  
Al/ Particulate silicon-reinforced aluminum  
SiC<sub>p</sub>-MMC matrix composite

BBD Box–Behnken's design  
RSM Response surface methodology  
SEM Scanning electron micrograph  
CS Cutting speed  
SR Surface roughness,  $R_a$  ( $\mu$ m)  
SG Spark gap  
Ip Peak current  
SV Spark gap voltage  
 $T_{on}$  Pulse on time  
 $T_{off}$  Pulse off time  
WF Wire feed rate  
WT Wire tension

Technical Editor: Márcio Bacci da Silva.

✉ Harmesh Kumar  
harmesh.kumar@bbsbec.ac.in

Alakesh Manna  
kgpmanna@rediffmail.com

Rajesh Kumar  
rajesh\_krs@rediffmail.com; rajesh\_krs@sliet.ac.in

<sup>1</sup> Department of Mechanical Engineering, Baba Banda Singh Bahadur Engineering College, Fatehgarh Sahib, Punjab 140406, India

<sup>2</sup> Department of Mechanical Engineering, PEC University of Technology (Formerly Punjab Engineering College), Chandigarh 160012, India

<sup>3</sup> Department of Mechanical Engineering, Sant Longowal Institute of Engineering and Technology, Longowal, Punjab 148106, India

## 1 Introduction

Particulate silicon carbide-reinforced aluminum matrix composite (Al/SiC<sub>p</sub>-MMC) has high strength-to-weight ratio, high stiffness, low thermal expansion coefficient, high thermal conductivity as well as corrosion and wear resistance [1–3]. These enhanced properties made Al/SiC<sub>p</sub>-

MMC a suitable alternate material for use in the industries such as aerospace, defense, automobile, electronic packaging and sports industries. But the presence of hard reinforced SiC particles makes machining of such material difficult by the traditional machining processes because of severe tool wear [3, 4]. Researchers have applied advanced machining processes such as electrochemical machining, abrasive jet machining, electric discharge machining and laser beam machining to machine aluminum metal matrix composites (Al-MMCs). Out of various advanced machining processes available, wire-cut electric discharge machining (WEDM) process emerged as an efficient and cost-effective process to machine Al-MMCs [5].

The workforce making use of the WEDM process is generally interested in higher workpiece cutting speed with the desired level of accuracy and surface finish. The performance of the WEDM process, however, is affected by many process parameters (i.e., pulse on time, pulse off time, peak current, spark gap voltage, wire tension, wire feed rate, flushing pressure and open gap voltage), and a single parameter change will influence the machining in a complex way. In the presence of many influencing parameters and stochastic nature of the process, achieving the optimal process performance is a challenge. An effective way to solve this problem is to investigate the relationship between response variables and its process parameters by modeling the process through suitable mathematical technique and followed by optimization using suitable optimization technique [6]. In the present work, response surface methodology (RSM) is used to model the input process parameters, whereas the optimal parametric setting is realized through traditional desirability function approach coupled with user's preference rating method. The user's preference rating method is a weight assignment method that resolves the issue of assigning weights to multiple responses taking into account the priorities of multiple users.

The next section illustrates the previous research on parametric analysis, modeling and optimization of WEDM process parameters.

## 2 Review of past research work

Several researchers carried out investigations for improving the response characteristics during WEDM of Al-MMCs. Yan et al. [7] studied WEDM of Al/Al<sub>2</sub>O<sub>3</sub>-MMC using one-factor-at-a-time strategy. The effect of the pulse on time and %volume fraction of Al<sub>2</sub>O<sub>3</sub>-reinforced particles on cutting speed, surface roughness,  $R_a$  (SR) and kerf width was studied. Tosun and Cogun [8] examined the effect of process parameters on wire wear ratio and modeled it statistically by using regression analysis techniques. They concluded that high wire wear ratio is always

accompanied by high material removal rate (MRR) and high SR values. Patil and Brahmkar [9] developed a semiempirical relation for MRR in WEDM of Al/SiC<sub>p</sub>-MMC applying dimension analysis and nonlinear estimation technique. In another communication [10], they presented investigation on the effect of electrical and non-electrical parameters on SR, cutting rate and kerf width making use of Taguchi design of the experiment. They applied multiple regression techniques to develop prediction models for the response variables separately. Shandilya et al. [11] compared artificial neural network and RSM methodologies based on prediction accuracy for average cutting speed in WEDM of Al/SiC<sub>p</sub>-MMC. Manna and Bhattacharyya [12] used Taguchi-based design of experiment (i.e., L-18 mixed orthogonal array) and S/N ratio for the parametric optimization in WEDM of Al/SiC<sub>p</sub>-MMC. They used Gauss elimination method for development of mathematical models. The investigations on WEDM of different Al-MMCs for single-response optimization were performed by Patel et al. [13], Shandilya et al. [14] and Pramanik et al. [15] and concluded that the WEDM can be efficiently utilized for machining of Al-MMCs.

It is revealed from the review of the literature on WEDM that researchers had defined an objective function in several ways to solve multi-response optimization problems. Milan et al. [16] used a simple weighing method to transform multi-responses, i.e., MRR and SR into a single response, and obtained the optimal parametric combination by utilizing artificial bee colony-based optimization. In the simple weighing method, the investigators generally assigned equal weights to response variables based on their own assumptions. Mahapatra and Patnaik [17] presented an investigation on optimization of WEDM process parameters using Taguchi design of the experiment. The authors applied the Genetic algorithm for multi-response optimization with the assignment of different combination of weights to response variables for overcoming the different machining situations arising out of user's requirement. Fard et al. [18] associated an artificial bee colony algorithm with adaptive neuro-fuzzy inference system models in order to maximize cutting speed and minimize SR, simultaneously during dry WEDM of Al/SiC<sub>p</sub>-MMC. In their work, the weights in the range of 0.6–0.9 and 0.1–0.4 are considered for cutting speed and SR, respectively, according to their importance in the process. They presented optimal solutions for various combinations of weights and discussed the effect of variation of weights on the response variables. In a similar way, Mahapatra and Patnaik [19] assigned weights to response variables during multi-response optimization of WEDM process parameters in machining of D2 tool steel using Taguchi design of experiments. Garg et al. [20] investigated machining characteristics and optimized WEDM process parameters during machining of newly

developed Al/ZrO<sub>2</sub>-MMC material making use of response surface methodology. They have assigned the weight in a random manner to the response variables. Prasad and Krishna [21] divided the problem as (a) optimization of kerf width with wire wear as a constraint and (b) optimization of wire wear with kerf width as a constraint. They arrived at the optimal parameters by applying harmony search algorithm-based optimization. Assarzadeh and Ghoreishi [22] used desirability function approach to optimize the process performance under each machining regime, i.e., finishing ( $R_a \leq 3 \mu\text{m}$ ), semi-finishing ( $3 \mu\text{m} < R_a < 4.5 \mu\text{m}$ ) and roughing ( $R_a > 4.5$ ). They presented sets of optimal solutions which make the MRR as high as possible and keep the SR within their specified range.

From the review of the literature, it is realized that most of the investigations in WEDM of Al/SiC<sub>p</sub>-MMC had been focused on parametric analysis and single-response optimization problems using Taguchi method. To the best of author's knowledge, only a few works have been reported on multi-response optimization in WEDM of Al/SiC<sub>p</sub>-MMC. It has also been observed that the investigators generally assign equal weights to response variables while defining objective function, based on their own assumptions or past experience. The assignment of weights, however, could be different for the responses as per the requirement. Additionally, if in a group, users have a difference of opinion over the weights of response variables, it becomes difficult to make decisions [23].

To deal with this situation, user's preference rating method has been applied in the present work for calculating the weights of response variables in order to satisfy the priorities of multiple users. Multi-response optimization has been done based on desirability function approach coupled with the user's preference rating for effective machining of Al/SiC<sub>p</sub>-MMC. Further, along with workpiece cutting speed (CS) and SR, the spark gap (SG) is also considered as the response variable in this work. The SG is an important response variable but was less investigated in the previous studies. The quadratic regression models have been developed for selected response variables in terms of six prominent input parameters using RSM. The study also investigates the machined surface in terms of surface topography and material diffusion between the wire electrode and workpiece material.

The next section depicts the development of quadratic regression models for the response variables in WEDM.

### 3 Modeling of WEDM parameters for response variables

The relationship between the controllable WEDM parameters and the output response variables has been quantified with the help of RSM. The six-factor-3-level Box–Behnken's design (BBD) has been utilized to plan the experiments. The BBD is very efficient in RSM for fitting the second-order model with a smallest possible number of experiments. The BBD has no points at the vertices of the cube defined by the ranges of the factors; that is, the design does not contain combinations where all the factors are at their higher or lower levels [24]. In the present study, BBD design consists of six parts; each carries eight runs. Within each part, three parameters are arranged in a full three-level factorial design, while the level of other parameters is set at zero (coded value). Therefore, the six-parameter BBD requires 48 runs plus the 6 number of replicates at the center point to estimate the pure error.

The chemical composition of the stir cast Al/SiC<sub>p</sub>-MMC used for the experimental work is shown in Table 1. Figure 1 shows the scanning electron micrograph (SEM) and corresponding spectra of energy-dispersive X-rays (EDX) of the Al/SiC<sub>p</sub>-MMC workpiece at two selected regions. The SEMs of the Al/SiC<sub>p</sub>-MMC were taken at accelerating voltage 20 kV and  $\times 100$  magnification. The EDX is a technique used to identify the elemental composition of a specimen. The spectrum-1 in the scanned region shows the presence and distribution of reinforced SiC particles in the aluminum matrix material. Spectrum-2 in the figure depicts the elemental analysis for the reinforcing phase. Peaks of silicon (Si) and carbon (C) indicate the presence of reinforced SiC particles in the matrix material.

Details of setups used in experimentation are given below:

- Machine type/make: sprintcut CNC-WEDM, Electronica
- Wire electrode: brass,  $\phi 250 \mu\text{m}$  diameter
- Dielectric fluid: deionized water (temperature 22–25 °C)
- Workpiece specification: cavity size: 5 mm  $\times$  5 mm  $\times$  15 mm, Al/SiC<sub>p</sub>-MMC (Stir cast)
- Surface roughness measuring device: Mitutoyo's surface roughness tester (S J 301)
- Spark gap measuring device: TESAMASTER micrometer (least count = 0.001 mm)

**Table 1** Composition of Al/SiC-MMC used for experiment

Type of MMC	Type of reinforced particle	%wt. SiC	% Cu	% Mg	% Si	% Fe	% Mn	% Ti	Remaining
Particulate MMC (Stir cast)	SiC (APS: 37 $\mu\text{m}$ )	10	0.02	0.628	0.492	0.32	0.12	0.01	Al

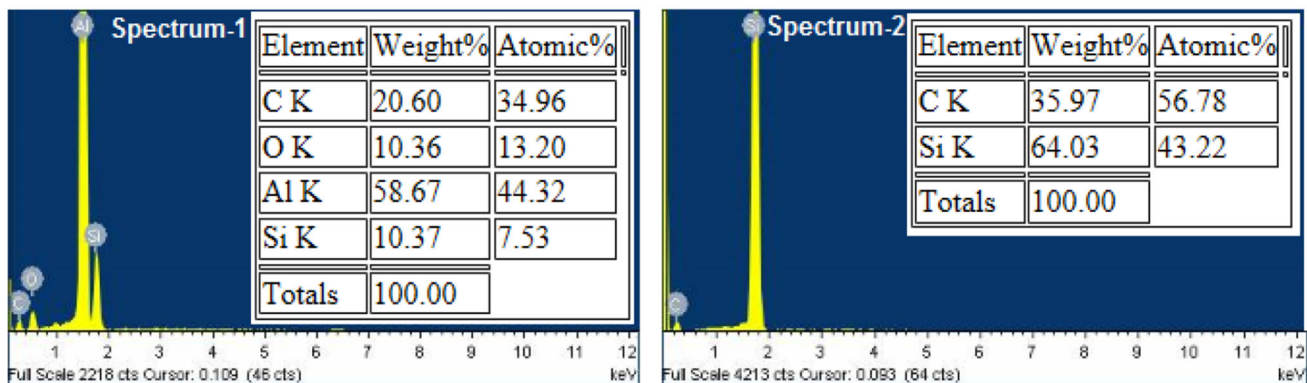
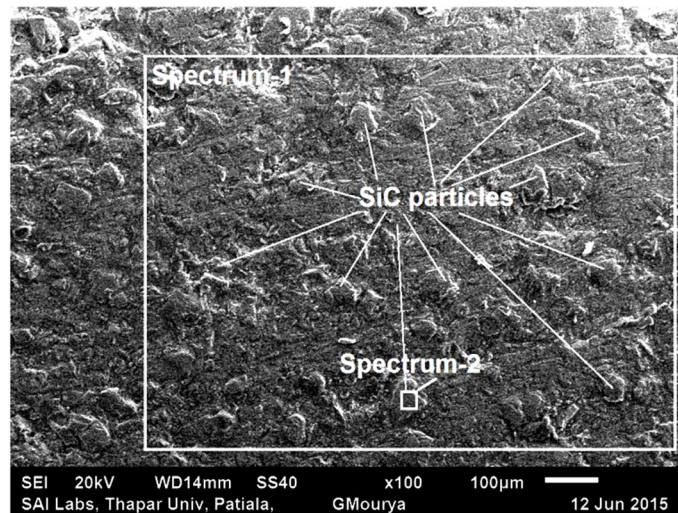


Fig. 1 SEM micrograph with EDX analysis of stir cast Al/SiC<sub>p</sub>-MMC at two selected regions (spectrum-1 selected region on Al/SiC<sub>p</sub>-MMC and spectrum-2 selected region on reinforced SiC particle)

The average CS was calculated for each experimental run by measuring the total area machined by the wire electrode and the required machining time [7]. The SR is measured at three chosen locations on each machined surface. The average values have been taken as test results and utilized for further analysis. The size obtained after machining (i.e., actual size) of workpiece was measured using a TESAMASTER micrometer. The SG was calculated from the relationship (Eq. 1) as follows:

$$\begin{aligned} & \text{Diameter of wire} + 2 (\text{spark gap}) \\ & = \text{geometrical size traced by the center of wire} \quad (1) \\ & - \text{size obtained after machining} \end{aligned}$$

To select the process parameters and their range during WEDM of Al/SiC<sub>p</sub>-MMC, the pilot experiments were conducted using one-factor-at-a-time approach. In this approach, experiments were performed by varying one parameter at a time keeping all other parameters at fixed levels. This approach is effective when emphasis is only to estimate main effects of the parameters on response variables especially during pilot experiments where it is desirable to identify the key parameters and their levels.

Range of the various controllable process parameters for detailed experiments was decided by analyzing the acquired pilot experiment data [25]. Table 2 shows the settings of six process parameters with their levels, units and notations as considered for experimentation. Table 3 shows the experimental matrix with results. A total of 54 experimental trials were conducted as per BBD in random order to avoid any systematic error creeping into the system. Figure 2 shows the photograph of machined workpieces.

Table 2 WEDM process parameters with their levels

S. no.	Parameter	Notation	Units	Level		
				- 1	0	1
1	Pulse on time	$T_{on}$	µs	0.6	0.9	1.2
2	Pulse off time	$T_{off}$	µs	16	22	28
3	Spark gap voltage	SV	V	20	30	40
4	Peak current	$I_p$	A	120	150	180
5	Wire tension	WT	g	850	1000	1200
6	Wire feed rate	WF	m/min	6	8	10

**Table 3** Design matrix with response values

Std. run no.	Machine input parameters						Response variables		
	$T_{on}$ ( $\mu$ s)	$T_{off}$ ( $\mu$ s)	SV (V)	$I_p$ (A)	WT (g)	WF (m/min)	CS ( $\text{mm}^2/\text{min}$ )	SR ( $R_a$ , $\mu$ m)	SG (mm)
<b>Part 1</b>									
1	0.6	16	30	120	1000	8	67.53	2.88	0.0407
2	1.2	16	30	120	1000	8	93.52	3.26	0.050
3	0.6	28	30	120	1000	8	35.48	2.85	0.034
4	1.2	28	30	120	1000	8	78.29	3.21	0.048
5	0.6	16	30	180	1000	8	71.64	3.04	0.042
6	1.2	16	30	180	1000	8	97.29	3.89	0.053
7	0.6	28	30	180	1000	8	48.73	3.08	0.041
8	1.2	28	30	180	1000	8	97.57	3.68	0.053
<b>Part 2</b>									
9	0.9	16	20	150	850	8	89.34	3.74	0.047
10	0.9	28	20	150	850	8	75.39	3.48	0.042
11	0.9	16	40	150	850	8	88.09	3.42	0.058
12	0.9	28	40	150	850	8	48	3.22	0.047
13	0.9	16	20	150	1200	8	95.68	3.28	0.045
14	0.9	28	20	150	1200	8	70.56	3.38	0.037
15	0.9	16	40	150	1200	8	90.34	3.18	0.045
16	0.9	28	40	150	1200	8	56.35	3.12	0.040
<b>Part 3</b>									
17	0.9	22	20	120	1000	6	87.67	3.48	0.046
18	0.9	22	40	120	1000	6	65.58	3.14	0.040
19	0.9	22	20	180	1000	6	99.63	3.62	0.044
20	0.9	22	40	180	1000	6	73.47	3.77	0.053
21	0.9	22	20	120	1000	10	90.43	3.48	0.037
22	0.9	22	40	120	1000	10	60.68	2.96	0.043
23	0.9	22	20	180	1000	10	96.83	3.7	0.042
24	0.9	22	40	180	1000	10	80.38	3.76	0.051
<b>Part 4</b>									
25	0.6	22	30	120	850	8	42.56	2.95	0.042
26	1.2	22	30	120	850	8	89.63	3.38	0.047
27	0.6	22	30	180	850	8	60.84	3.31	0.045
28	1.2	22	30	180	850	8	99.84	3.83	0.054
29	0.6	22	30	120	1200	8	45.58	2.75	0.034
30	1.2	22	30	120	1200	8	84.38	3.07	0.045
31	0.6	22	30	180	1200	8	60.37	3.02	0.036
32	1.2	22	30	180	1200	8	96.78	3.62	0.054
<b>Part 5</b>									
33	0.9	16	30	150	850	6	94.18	3.79	0.052
34	0.9	28	30	150	850	6	62.93	3.35	0.045
35	0.9	16	30	150	1200	6	87.73	3.42	0.047
36	0.9	28	30	150	1200	6	77.38	3.38	0.036
37	0.9	16	30	150	850	10	92.35	3.68	0.048
38	0.9	28	30	150	850	10	64.14	3.47	0.045
39	0.9	16	30	150	1200	10	90.89	3.19	0.044
40	0.9	28	30	150	1200	10	67.04	3.24	0.039
<b>Part 6</b>									
41	0.6	22	20	150	1000	6	47.92	3.08	0.033

**Table 3** (continued)

Std. run no.	Machine input parameters						Response variables		
	$T_{on}$ ( $\mu$ s)	$T_{off}$ ( $\mu$ s)	SV (V)	Ip (A)	WT (g)	WF (m/min)	CS ( $\text{mm}^2/\text{min}$ )	SR ( $R_a$ , $\mu$ m)	SG (mm)
42	1.2	22	20	150	1000	6	104.45	3.89	0.047
43	0.6	22	40	150	1000	6	48.25	2.89	0.039
44	1.2	22	40	150	1000	6	82.56	3.64	0.052
45	0.6	22	20	150	1000	10	48.38	3.01	0.033
46	1.2	22	20	150	1000	10	96.29	3.76	0.047
47	0.6	22	40	150	1000	10	46.59	2.83	0.042
48	1.2	22	40	150	1000	10	84.78	3.36	0.054
Central points									
49	0.9	22	30	150	1000	8	73.54	3.35	0.039
50	0.9	22	30	150	1000	8	72.48	3.36	0.040
51	0.9	22	30	150	1000	8	80.82	3.41	0.042
52	0.9	22	30	150	1000	8	72.38	3.32	0.041
53	0.9	22	30	150	1000	8	79.25	3.3	0.042
54	0.9	22	30	150	1000	8	76.64	3.4	0.0385

To study the effect of WEDM parameters, i.e., pulse on time, pulse off time, peak current, spark gap voltage, wire tension and wire feed rate on response variables, i.e., CS, SR and SG, a second-order response model is fitted into the following equation:

$$y = \beta_0 + \sum_{i=1}^k \beta_i x_i + \sum_{i=1}^k \beta_{ii} x_i^2 + \sum_{i < j} \beta_{ij} x_i x_j \quad (2)$$

Here,  $y$  is a response variable and  $x_i$  and  $x_j (1, 2, \dots, k)$  are  $k$  input controllable process parameters. The coefficient  $\beta_0$  is the free term, the coefficients  $\beta_i$  are the linear terms, the coefficients  $\beta_{ii}$  are the quadratic terms, and the coefficients  $\beta_{ij}$  are the

interaction terms [24]. Equations for CS, SR and SG are then derived, by determining the values of the coefficients using the least square techniques for the data collected in 54 experimental trials as shown in Table 3 and presented as follows:

$$\begin{aligned} \text{Cutting speed (CS)} = & 46.44222 + 207.46667 * T_{on} \\ & - 2.23417 * T_{off} + 2.06279 * SV \\ & - 1.08328 * IP - 89.88426 * T_{on}^2 \\ & + 4.26852E-003 * IP^2 + 2.77847 \\ & * T_{on} * T_{off} - 1.33083 * T_{on} * SV \\ & - 0.072938 * T_{off} * SV \end{aligned} \quad (3)$$

$$\begin{aligned} \text{Surface Roughness (SR)} = & 7.49549 + 2.56399 T_{on} \\ & - 0.073857 T_{off} \\ & - 0.077750 SV - 0.013306 Ip \\ & - 2.11263E-003 WT \\ & - 0.36366 WF - 1.51703 T_{on}^2 \\ & + 0.021335 WF^2 \\ & + 7.50000E-003 T_{on} Ip \\ & + 6.32883E-005 T_{off} WT \\ & + 4.45833E-004 SV Ip \end{aligned} \quad (4)$$

$$\begin{aligned} \text{Spark gap (SG)} = & 0.21209 - 0.012017 * T_{on} \\ & - 2.32801E-003 * T_{off} \\ & - 8.83333E-004 * SV \\ & - 7.47551E-004 * IP \\ & - 1.47797E-004 * WT \\ & + 4.26031E-005 * T_{off}^2 \\ & + 2.00758E-006 * IP^2 \\ & + 5.00325E-008 * WT^2 \\ & + 3.17114E-005 * T_{on} * WT \\ & + 7.58333E-006 * SV * IP \end{aligned} \quad (5)$$

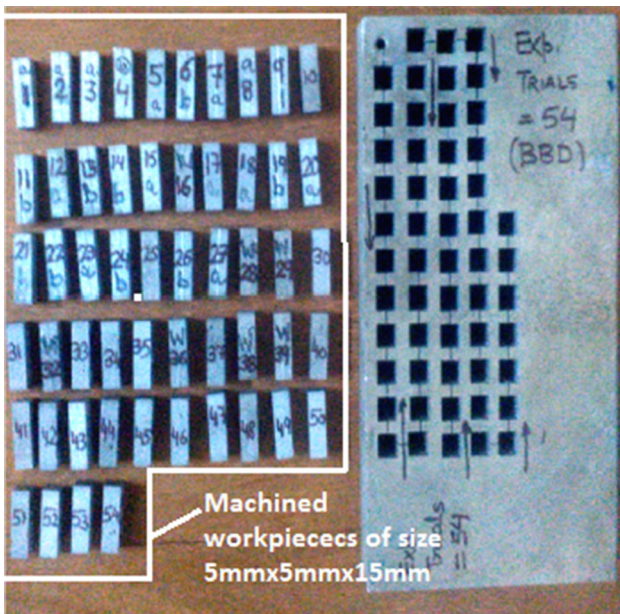


**Fig. 2** Photograph of machined workpieces

**Table 4** ANOVA test for cutting speed, surface roughness ( $R_a$ ) and spark gap

Source	Sum of squares	DF	Mean square	F value	Prob > F	R-square
Analysis of variance for cutting speed						
Model	16223.15	9	1802.57	77.68	< 0.0001	$R^2 = 0.940$
$T_{on}$	9660.50	1	9660.50	416.30	< 0.0001	Adj $R^2 = 0.905$ Pred $R^2 = 0.928$
$T_{off}$	3190.58	1	3190.58	137.49	< 0.0001	Adeq Precision = 36.19
SV	1312.76	1	1312.76	56.57	< 0.0001	
Ip	840.64	1	840.64	36.23	< 0.0001	
$(T_{on})^2$	732.94	1	732.94	31.58	< 0.0001	
$(T_{off})^2$	165.29	1	165.29	7.12	0.0106	
$T_{on} \cdot T_{off}$	200.10	1	200.10	8.62	0.0053	
$T_{on} \cdot SV$	127.52	1	127.52	5.50	0.0236	
$T_{off} \cdot SV$	153.21	1	153.21	6.60	0.0136	
Residual	1021.04	44	23.21			
Lack of fit	955.12	39	24.49	1.86	0.2540	
Pure error	65.92	5	13.18			
Analysis of variance for surface roughness ( $R_a$ )						
Model	4.47	11	0.41	66.19	< 0.0001	$R^2 = 0.945$
$T_{on}$	1.98	1	1.98	322.86	< 0.0001	Adj $R^2 = 0.931$
$T_{off}$	0.070	1	0.070	11.32	0.0016	Pred $R^2 = 0.907$
SV	0.28	1	0.28	46.19	< 0.0001	Adeq Precision = 33.45
Ip	1.00	1	1.00	163.48	< 0.0001	
WT	0.39	1	0.39	62.69	< 0.0001	
WF	0.048	1	0.048	7.76	0.0080	
$(T_{on})^2$	0.24	1	0.24	38.81	< 0.0001	
$(WF)^2$	0.093	1	0.093	15.16	0.0003	
$T_{on} \cdot Ip$	0.073	1	0.073	11.86	0.0013	
$T_{off} \cdot WT$	0.071	1	0.071	11.58	0.0015	
SV · Ip	0.14	1	0.14	23.29	< 0.0001	
Residual	0.26	42	6.144E-003			
Lack of fit	0.25	37	6.667E-003	2.92	0.1159	
Pure error	0.011	5	2.280E-003			
Analysis of variance for spark gap						
Model	1.691E-003	10	1.691E-004	28.84	< 0.0001	$R^2 = 0.870$
$T_{on}$	8.829E-004	1	8.829E-004	150.60	< 0.0001	Adj $R^2 = 0.8401$ Pred $R^2 = 0.7898$
$T_{off}$	1.777E-004	1	1.777E-004	30.31	< 0.0001	Adeq Precision = 22.64
SV	1.550E-004	1	1.550E-004	26.45	< 0.0001	
Ip	1.460E-004	1	1.460E-004	24.91	< 0.0001	
WT	2.048E-004	1	2.048E-004	34.93	< 0.0001	
$(T_{off})^2$	2.588E-005	1	2.588E-005	4.41	0.0416	
$(Ip)^2$	4.104E-005	1	4.104E-005	7.00	0.0113	
$(WT)^2$	2.455E-005	1	2.455E-005	4.19	0.0469	
$T_{on} \cdot WT$	2.248E-005	1	2.248E-005	3.83	0.0567	
SV · Ip	4.141E-005	1	5.863E-006	7.06	0.0110	
Residual	2.521E-004	43	5.863E-006			
Lack of fit	2.406E-005	38	6.331E-006	2.75	0.1295	
Pure error	1.149E-005	5	2.299E-006			

Table 4 depicts the corresponding analysis of variance (ANOVA). To test whether the data are well fitted in

models or not, the calculated '*p values*' for all the prediction models are obtained to be less than 0.05 (i.e., 95% confidence level), indicating that developed models are

significant. The ' $R^2$ ' value represents the proportion of variation in the response explained by the regression model. The values of ' $R^2$ ' for Eqs. (3), (4) and (5) are 0.94, 0.94 and 0.87, respectively, which clearly indicate the significance of prediction models. Additionally, the developed models for selected responses have been checked using residual analysis. The residual plots for response variables CS, SR and SG are given in Figs. 3a, 4a and 5a, respectively. The 'Fat pencil thickness test' has been shown for a quick visual assessment of normality of data.

From these figures, it is observed that there is no severe departure from normality. As a whole, analysis of normal plots of residuals of selected responses, the models do not reveal inadequacy. Using the above models, the experimental and predicted data are plotted in Figs. 3b, 4b and 5b for CS, SR and SG, respectively. These figures clearly indicate that the predictions made by the regression models are in good conformity with the experimental values. Adequate precision ('Adeq Precision') measures the signal-to-noise ratio and are well above '4' in all models which is desirable (Table 4). Hence, it can be concluded that developed models are useful in predicting the selected response variables.

These models hence developed will provide an effective guideline to select the parametric settings for achieving desired CS, SR and SG during WEDM of Al/SiC<sub>p</sub>-MMC. The selection of proper parameters will help to reduce the manufacturing cost, improve product quality and increase productivity. These models are valid for machining of Al/10wt%SiC<sub>p</sub>-MMC on Sprintcut WEDM machine tool for the specified range of input process parameters. The knowledge of SG is essential to achieve the desired level of dimensional accuracy during shop floor machining. If the SG for a given parameter set is known in advance (i.e., using Eq. 5), that can be used for estimating the wire offset setting, thereby getting a dimensionally accurate product. Hence, these models could be very useful for the machinists on the shop floor for effective machining of Al/SiC<sub>p</sub>-MMC.

The next section briefly describes the multi-response optimization considering multiple users preference.

## 4 Multi-response optimization

Multi-response optimization implemented in the present work is based on desirability function approach coupled with user's preference rating method. Desirability function approach can solve multi-response optimization problem by converting it into single-response optimization problem. It provides flexibility to the investigators in assigning different weight to the responses as per the requirements in

terms of the product quality, productivity and acceptability of the product.

### 4.1 Calculation of weights by user preference rating method

The user's preference rating method has been applied for resolving the issue of assigning weights to multiple responses taking into account of conflicting interests of multiple users. The present work considers the viewpoints of four different users who have a different opinion on the weights of response variables. The preferences for each user have been represented in preferences graph (PG) as shown in (Fig. 6). The following steps have been followed for the calculation of weights [23].

#### (a) Adjacency matrix

The relationship shown in user's PG (Fig. 6) is transformed in a matrix form, known as an adjacency matrix. An adjacency matrix can be expressed as

$$PG_n = [pg_{ij}]_{M \times M} \quad (i, j = 1, 2, \dots, M) \quad (6)$$

where  $n$  is the number of users,  $M$  is number of responses, and  $pg_{ij}$  gives the dominance of  $i$  over  $j$  in a  $M \times M$  matrix.

Using Eq. (6), adjacency matrices are calculated as

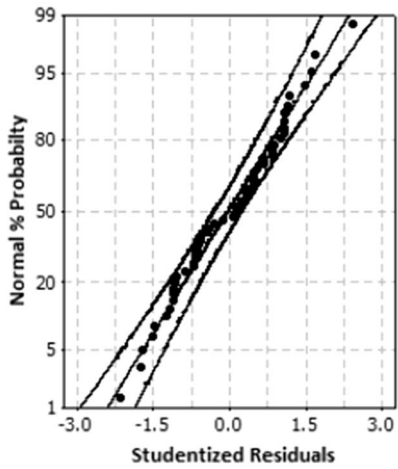
$$\begin{array}{l} \begin{array}{ccc} \text{CS} & \text{SR} & \text{SG} \\ PG_1 = & \begin{array}{ccc} 0 & 0 & 1 \\ 0 & 0 & 1 \\ 0 & 0 & 0 \end{array} & \begin{array}{l} \text{CS} \\ \text{SR} \\ \text{SG} \end{array} \\ & \begin{array}{ccc} 0 & 1 & 0 \end{array} & \\ PG_2 = & \begin{array}{ccc} 0 & 0 & 0 \\ 0 & 1 & 0 \\ 0 & 1 & 0 \end{array} & \\ PG_3 = & \begin{array}{ccc} 0 & 0 & 1 \\ 0 & 0 & 0 \\ 0 & 0 & 0 \end{array} & \\ PG_4 = & \begin{array}{ccc} 0 & 0 & 1 \\ 1 & 0 & 0 \end{array} & \end{array} \end{array}$$

#### (b) Dominance matrix

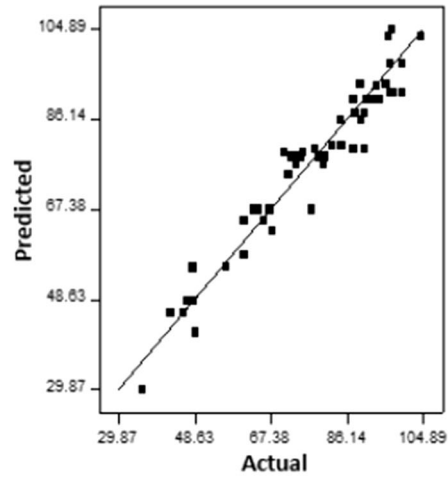
The dominance matrix ( $D^n$ ) is formed with the help of adjacency matrix. It is expressed as

$$D^n = PG_n^1 + PG_n^2 + \dots + PG_n^m + PG_n^{M-1} \quad (7)$$

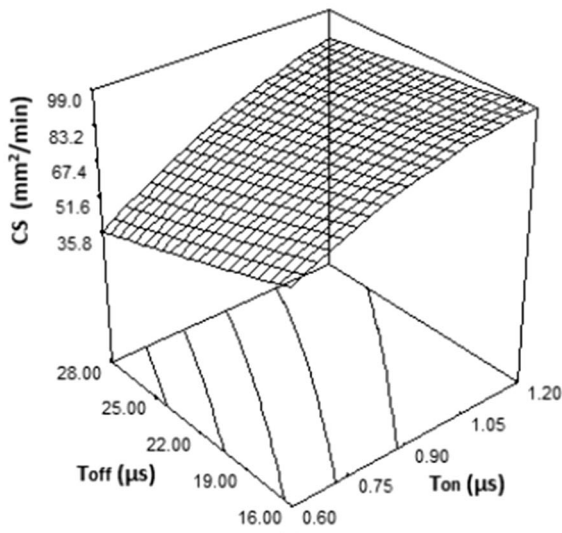




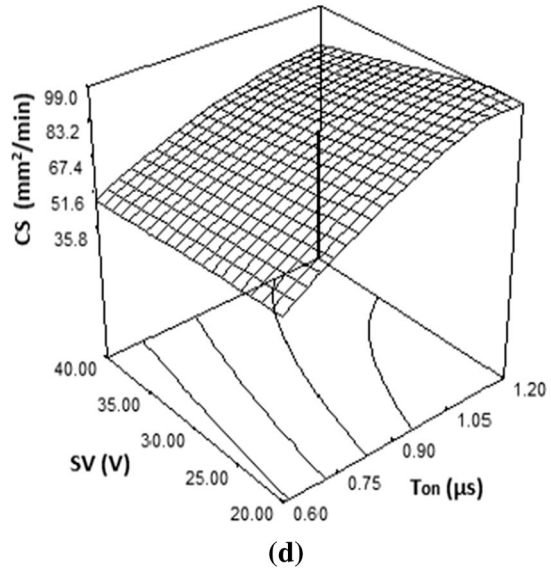
(a)



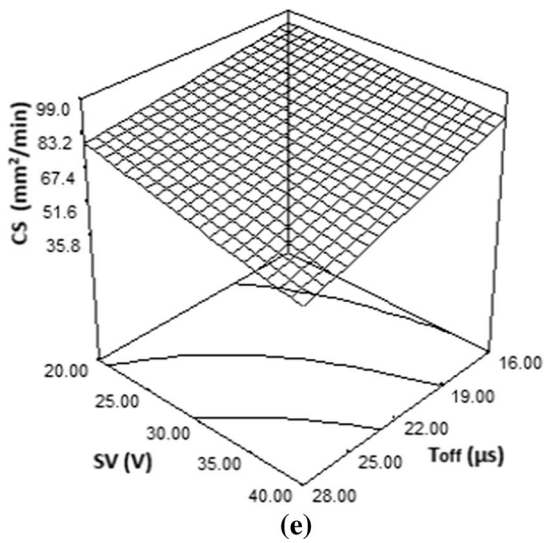
(b)



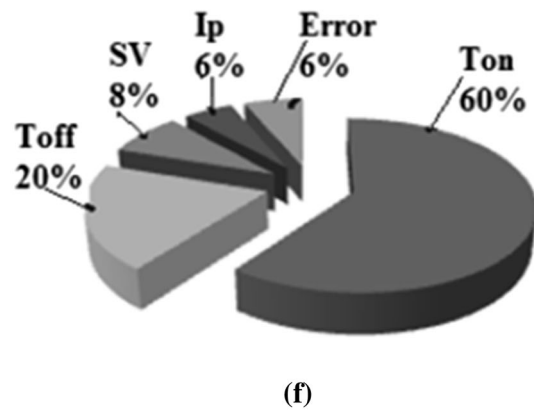
(c)



(d)



(e)



(f)

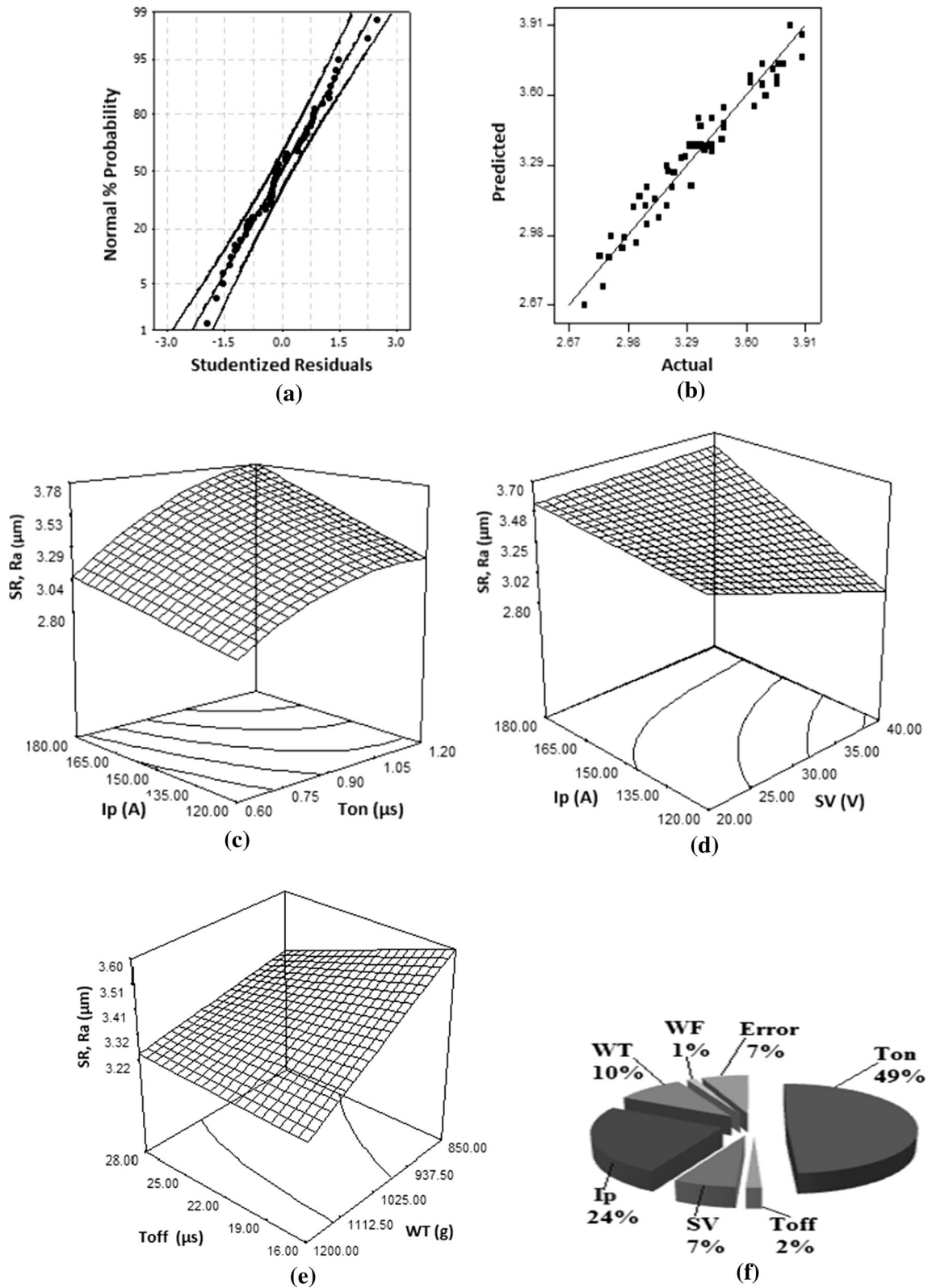


**Fig. 4** Residuals and response surface plots for surface roughness ( $R_a$ ) through response surface modeling. **a, b** Residuals plots, **c–e** response surface plots, **f** contribution of significant parameters

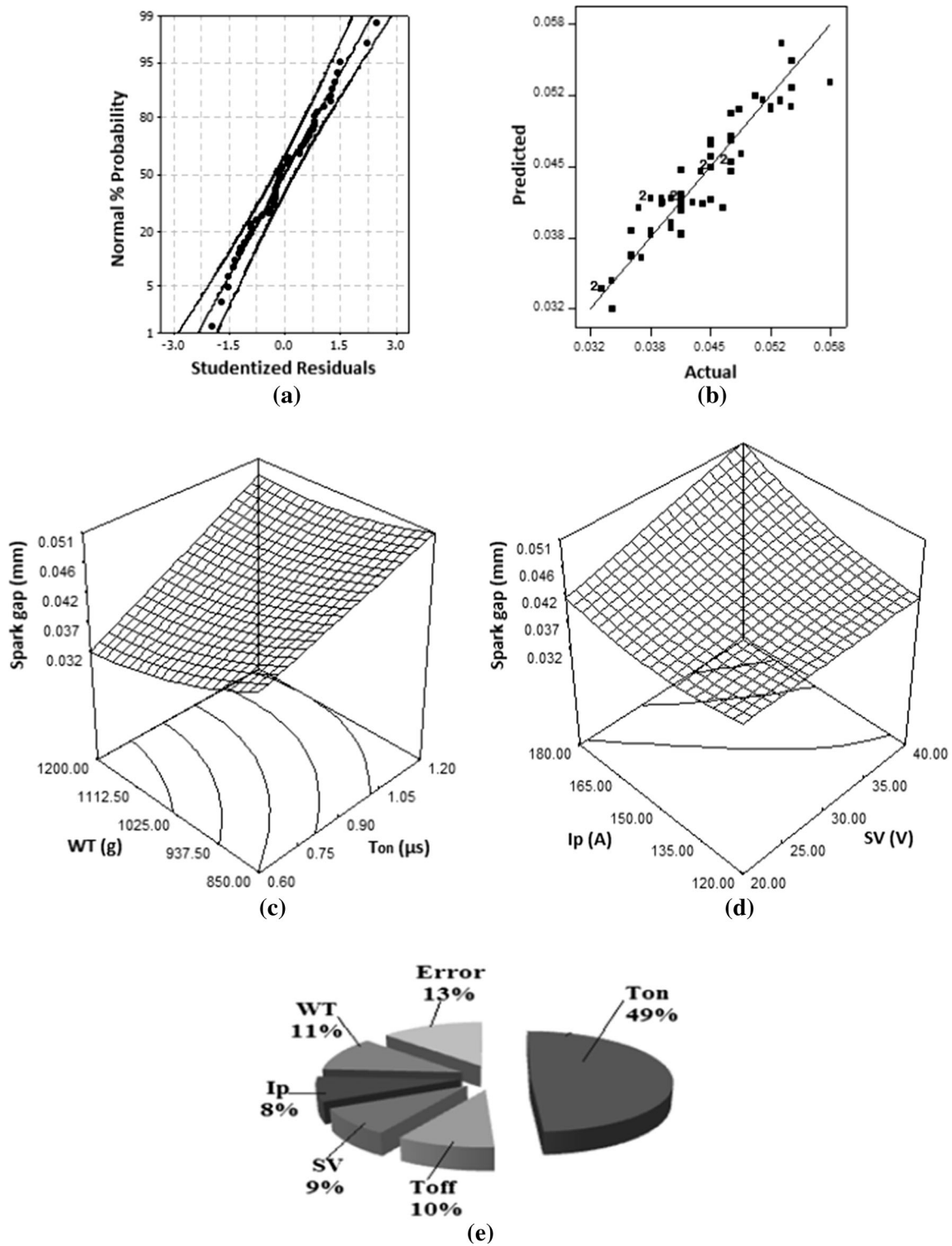
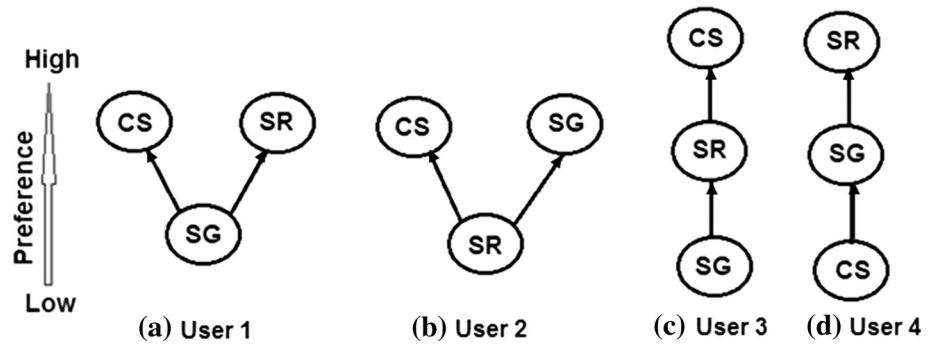


**Fig. 5** Residuals and response surface plots for spark gap through response surface modeling. **a, b** Residuals plots, **c, d** response surface plots, **e** contribution of significant parameters

**Fig. 6** Preference graphs for representing relative importance of response variables



Also  $d_m^n = \sum_{j=1}^M pg_{mj}$  where  $d_m^n$  represents the sum of entries ( $pg_{mj}$ ) in row  $m$  of dominance matrix. Using Eq. (7), the dominance matrices are calculated as

$$\begin{aligned}
 D_1 &= \begin{matrix} 0 & 0 & 1 \\ 0 & 0 & 1 \\ 0 & 0 & 0 \\ 0 & 1 & 0 \end{matrix} = \begin{matrix} 1 \\ 1 \\ 0 \\ 1 \end{matrix} \\
 D_2 &= \begin{matrix} 0 & 0 & 0 \\ 0 & 0 & 0 \\ 0 & 1 & 0 \\ 0 & 1 & 1 \end{matrix} = \begin{matrix} 0 \\ 0 \\ 1 \\ 2 \end{matrix} \\
 D_3 &= \begin{matrix} 0 & 0 & 1 \\ 0 & 0 & 0 \\ 0 & 0 & 0 \\ 0 & 0 & 0 \end{matrix} = \begin{matrix} 1 \\ 0 \\ 0 \\ 0 \end{matrix} \\
 D_4 &= \begin{matrix} 1 & 0 & 1 \\ 1 & 0 & 0 \end{matrix} = \begin{matrix} 2 \\ 1 \end{matrix}
 \end{aligned}$$

(c) Relative degree of performance

The relative degree of performance (RDP) exhibits the weightage of preference of the responses, in the scaled form (i.e., 0 to 1) by taking into account the preference of each user. It is shown by the following equation:

$$RDP_m^n = \frac{(1 + d_m^n)}{\max_{m=1 \dots M} (1 + d_m^n)} \tag{8}$$

Using Eq. (8), RDP for each user can be given by

$$RDP1 = (1, 1, 0.5); RDP2 = (1, 0.5, 1); RDP3 = (1, 0.66, 0.33); RDP4 = (0.33, 1, 0.66)$$

(d) Relative importance rating

The relative importance rating (RIR) represents the combined rating of single-response characteristics taking into account the views of four users. It can be expressed as

$$RIR_m = \frac{\sum_{n=1}^N RDP_m^n}{\max_{m=1 \dots M} \sum_{n=1}^N RDP_m^n} \tag{9}$$

The relative importance ratings for CS, SR and SG derived from Eq. (9) can be given by

$$RIR = (3.33/4, 3.16/4, 2.49/4) = (0.833, 0.790, 0.622)$$

(e) Weight computation

The weight of each response characteristics is calculated by using the following Eq. (10)

$$\begin{aligned}
 w_m &= \frac{RIR_m}{\sum_{m=1}^N RIR_m} \\
 w_m &= (0.833/2.244, 0.790/2.244, 0.622/2.244) \\
 &= (0.370, 0.352, 0.277)
 \end{aligned} \tag{10}$$

The user preference rating for different response variables such as CS, SR and SG are 0.371, 0.352 and 0.277, respectively, considering conflicting interests of multiple users.

**4.2 Desirability function approach**

In the present work, CS, SR and SG have been considered as response variables. It is observed that with the increase in CS, the other response variables SR and SG also increase. However, in machining, the optimal parametric setting should produce the maximum CS along with minimum SR and SG. A single-response optimization will not serve any purpose, as these objectives are conflicting in nature. In this study, the selected response variables have been optimized simultaneously using the developed models, i.e., Equations 8, 9 and 10, based on desirability function approach. The detail of this method is given in [24]. This method makes use of overall desirability function,  $D_o$ , as an objective function, and transforms individual responses into a scale-free value ( $D_i$ ) called individual desirability. The optimization is accomplished in the following steps:

- (a) Compute the individual desirability value ( $D_i$ ) for the selected responses using the formula proposed by the ‘Derringer and Suich’ that varies over the range  $0 \leq D_i \leq 1$ . The highest value in the range is one which represents the ideal case; zero indicates that one or more responses are outside their acceptable limits.
- (b) Calculate the overall desirability ( $D_o$ ). The individual desirability values of all the responses can be

combined to form a single value in the form of overall desirability ( $D_o$ ) by the following Eq. (11)

$$D_o = (D_1^{w_1} \times D_2^{w_2} \times \dots \times D_n^{w_n})^{1/n} = \left( \prod_{i=1}^n D_i^{w_i} \right)^{1/n} \tag{11}$$

where  $n$  is the number of response variables under consideration and  $w_i$  reflects the weight (relative importance) of different response characteristics. The weight,  $w_i$ , must satisfy the conditions  $0 < w_i < 1$  and  $\sum_{i=1}^n w_i = 1$ . Weights may be assigned according to the relative importance of responses in the multi-response optimization.

- (c) Maximize the overall desirability and identify the optimal parametric setting. The higher overall desirability value ( $D_o$ ) implies better overall performance of the process. The parametric setting with maximum overall desirability is considered to be the optimal parametric combination.

Utilizing the weights calculated by user’s preference rating method and according to Eq. (11), the overall desirability function is expressed as

$$D_o = (D_{CS}^{0.371} \times D_{SR}^{0.352} \times D_{SG}^{0.277})^{1/3} \tag{12}$$

The range of response variables and the goal and weights of the selected responses, e.g., CS, SR and SG, are shown in Table 5. The objective in the present case is to find out optimal parametric setting of process parameters which maximizes the overall desirability function (i.e., Equation 12). Minitab-16 software has been used for multi-response optimization of WEDM parameters. Figure 7 represents the optimization plot which shows how the parameters affect the predicted responses and also the optimization results. The vertical lines on the graph represent the current parametric setting, and horizontal dash lines represent the current values of response variables. Three optimal parametric settings of input process parameters for maximum overall composite desirability are reported in Table 6. The current optimal parametric settings are: pulse on time 0.75  $\mu$ s, pulse off time 16  $\mu$ s, spark gap voltage 35 V, peak current 120A, wire tension 1200 g and wire feed rate 10 m/min in machining of Al/SiC<sub>p</sub>-MMC considering the preference of multiple users.

A set of confirmation runs have been performed at optimal parametric settings, and their average values were computed for each response variables. As per the machine

**Table 5** Desirability analysis for cutting speed, surface roughness ( $R_a$ ) and spark gap

Response	Goal	Lower Limit	Upper Limit	Weight	Importance
Cutting speed (mm <sup>2</sup> /min)	Maximize	70	110	1	0.371
Surface roughness, $R_a$ ( $\mu$ m)	Minimize	2.4	3.5	1	0.362
Spark gap (mm)	Minimize	0.035	0.045	1	0.277

**Fig. 7** Multi-response optimization plot for optimal performance

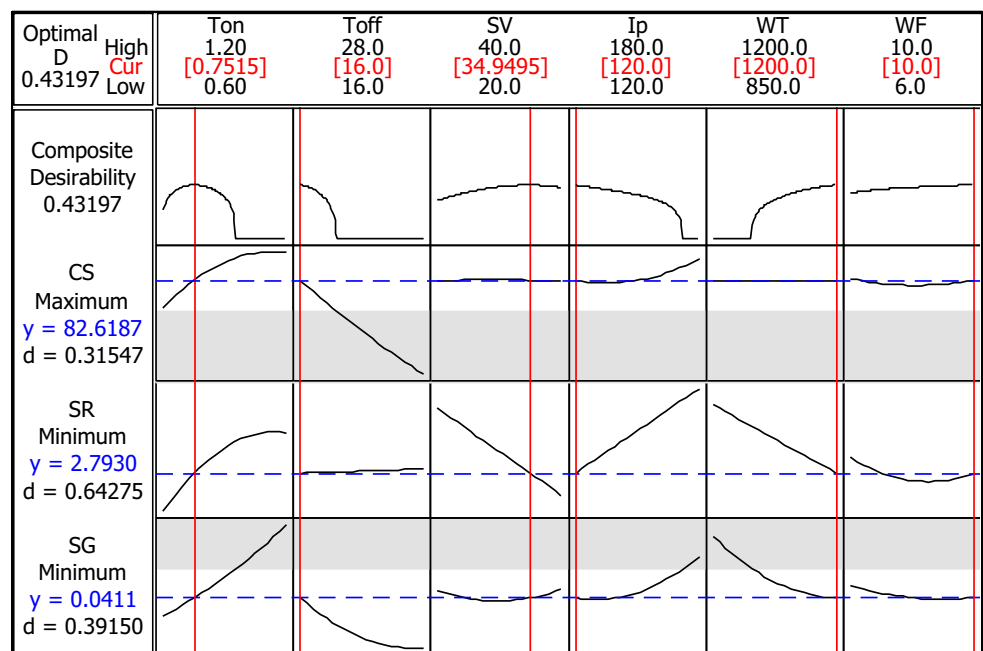


**Table 6** Optimization results through desirability functions approach

Sol. no.	Machine input parameters						Responses			Composite desirability
	$T_{on}$ ( $\mu$ s)	$T_{off}$ ( $\mu$ s)	SV (V)	$I_p$ (A)	WT (g)	WF (m/min)	CS ( $\text{mm}^2/\text{min}$ )	SR ( $\mu$ m)	SG (mm)	
1	0.75	16	35	120	1200	10	82.61	2.79	0.0411	0.432
2	0.83	16	39.87	120	1200	9.67	80.28	2.72	0.0416	0.397
3	0.78	16	20	180	1200	8.35	93.24	3.23	0.0409	0.385

**Table 7** Confirmation experiments and results

Sol no.	Modified input parameters						Experimental			Predicted			Prediction error (%)		
	$T_{on}$ ( $\mu$ s)	$T_{off}$ ( $\mu$ s)	SV (V)	$I_p$ (A)	WT (g)	WF (m/min)	CS ( $\text{mm}^2/\text{min}$ )	SR ( $\mu$ m)	SG (mm)	CS ( $\text{mm}^2/\text{min}$ )	SR ( $\mu$ m)	SG (mm)	CS ( $\text{mm}^2/\text{min}$ )	SR ( $\mu$ m)	SG (mm)
1.	0.75	16	35	120	1200	10	78.32	2.70	0.043	82.61	2.79	0.041	5.47	3.33	4.65
2.	0.85	16	40	120	1200	10	86.08	2.72	0.040	81.94	2.77	0.042	4.82	1.85	4.38
3.	0.8	16	20	180	1200	8	97.39	3.37	0.042	94.63	3.26	0.041	2.84	3.43	2.87

and hardware constraints, the confirmation tests have been performed with the nearest available parametric setting value to the optimum one (Tables 6 and 7). The values of CS, SR and SG predicted through models (Eqs. 3, 4 and 5) and obtained by confirmation runs are presented in Table 7. From the analysis of Table 7, it can be observed that the prediction error is very less. The percentage absolute error between experimental and predicted values at the optimal settings of WEDM parameters for selected responses is less than 5.5%. This confirms excellent reproducibility of the experimental conclusions.

The next section describes the parametric effects on selected response variables and the analysis of machined surface.

## 5 Parametric effects on response variables

The parametric analysis has been carried out to study the influence of the input process parameters such as pulse on time, pulse off time, peak current, spark gap voltage, wire tension and wire feed rate on response variables, i.e., CS, SR and SG in WEDM of Al/SiC<sub>p</sub>-MMC. Response surface using quadratic regression models has been plotted to assess the change of response surface.

### 5.1 Parametric effects on cutting speed

Based on RSM model, the effects of the pulse on time and pulse off time on CS, while keeping other parameters at the center level, are shown in Fig. 3c. The nonlinear nature of variation of CS with parameter pulse on time has been observed. From the figure, it is clear that

increasing pulse on time leads to an increase in cutting speed for all setting values of pulse off time. Figure 8 compares the SEM of the machined surface generated under two experimental trials. By comparing Fig. 8a, b at the same magnification, it is observed that higher pulse on time and lower pulse off time generate high discharge energy, which results in the development of larger, deeper and overlapped craters on the machined surface. This, in turn, will remove more volume of material from the workpiece resulting in higher cutting speed. The results are in agreement with the work of Rao and Krishna [26], and Satishkumar et al. [27].

Response surface of CS versus spark gap voltage and pulse on time is presented in Fig. 3d. At the lower spark gap voltage, it can be observed that the CS increases sharply with the pulse on time. The increase in CS, however, becomes gradual at higher spark gap voltage. The lower spark gap voltage narrows the gap between the workpiece and wire electrode which results in increase in the number of sparks produced leading to the increased metal removal and hence higher CS. Figure 3e shows the effects of pulse off time and spark gap voltage on CS. From the figure, it can be noticed that lower pulse off time and lower spark gap voltage combination results in higher CS due to higher pulse frequency. In this parametric setting, higher thermal energy gets transferred from wire electrode to workpiece. The non-cutting time during machining is reduced at smaller pulse off time. This, in turn, will increase the pulse frequency leading to better CS. However, application of the too low value of pulse off time has an arcing tendency during machining resulting in wire breakage. It can be noticed that both pulses off time and spark gap voltage have linear nature of variation for CS.

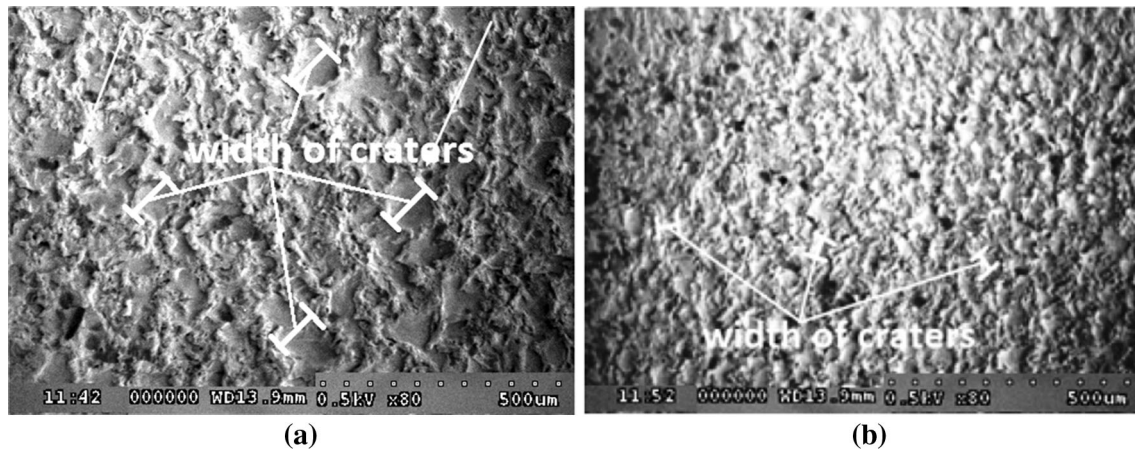


**Fig. 8** SEM micrographs ( $\times 80$ ) of machined surface of Al/SiC<sub>p</sub>-MMC under two test conditions **a.** Run.2-  $T_{on} = 1.2 \mu s$   $T_{off} = 16 \mu s$   $SV = 30 V$   $I_p = 120A$   $WT = 1000 g$   $WF = 8 m/min$ , **b.** Run.3-  $T_{on} = 0.6 \mu s$   $T_{off} = 28 \mu s$   $SV = 30 V$   $I_p = 120A$   $WT = 1000 g$   $WF = 8 m/min$

The results are corresponding to the work of Satishkumar et al. [27].

The percentage contribution of significant process parameters on *CS* is shown in Fig. 3f. Referring to the sum of squares in Table 4, the parameter pulse on time makes the largest contribution to the total sum of squares  $[(9660.5/16025.52) \times 100 = 60.2\%]$ . The pulse off time makes the next largest contribution (20%), whereas the parameters spark gap voltage and peak current together make only 14% contributions. The parameters wire tension and wire feed rate have no significant effect on *CS*.

## 5.2 Parametric effects on surface roughness, $R_a$

The effects of the pulse on time and peak current on *SR* are shown in Fig. 4c. It can be seen that lower pulse on time and lower peak current combination results in lower *SR* due to lower discharge energy in machining which produces small and shallower discharge crater on the machined surface. The same is verified from the SEM in Fig. 8b. This parametric combination causes lesser deterioration of machined surface. Also, the surface irregularities are found to be less frequent. The results are in agreement with work of Patil and Brahmanekar [10], Rao and Krishna [26] and Satishkumar et al. [27].

Figure 4d shows the variation in *SR* with pulse off time and wire tension. It can be seen from the figure that higher wire tension and higher pulse off time combination results in lower *SR*. This is because increasing wire tension decreases the chances of wire deflection and vibration during machining which results in stable machining; therefore, it produces better surface finish on the machined surface. Further, an increase in pulse off time increases the non-cutting time and hence better flushing of debris and dislodged reinforced SiC particle from machining zone. The results are in agreement with the work reported by

Patil and Brahmanekar [10] but are contrary to the work reported by Rao and Krishna [26]. The results might have differed due to the variation in the size of reinforced SiC particles used in their work. The effects of spark gap voltage and peak current on *SR* are shown in Fig. 4e. It can be seen that lower peak current and higher spark gap voltage combination results in the better surface finish. In this machining condition, small and shallower craters are formed on the machined surface [28].

The percentage contribution of significant parameters on *SR* is shown in Fig. 4f. Pulse on time is the major parameter affecting the *SR*, i.e., 49%. The percentage contribution of peak current, wire tension and spark gap voltage on *SR* is 24%, 10%, and 7%, respectively.

## 5.3 Parametric effects on the spark gap

The effects of the pulse on time and wire tension on *SG* are shown in Fig. 5c. The linear nature of variation of *SG* with a pulse on time has been observed. The *SG* increases with the increase in pulse on time for all setting values of wire tension. It can be seen that lower pulse on time and higher wire tension combination results in lower spark gap. This is due to the fact that the volume of material removed is less at smaller pulse on time due to the less thermal energy released in the machining gap. On the other hand, an increase in wire tension avoids wire deflection and vibrations from its straight path which causes stable machining (i.e., least fluctuation in actual spark gap voltage during machining), thereby producing lower *SG*. It can be noticed that lowest pulse on time (0.6  $\mu s$ ) and highest wire tension (1200 g) are needed to get minimum value of *SG*. The results are in agreement with the work of Patil and Brahmanekar [10].

The investigation of possible surface and subsurface defects due to improper selection of machining parameters

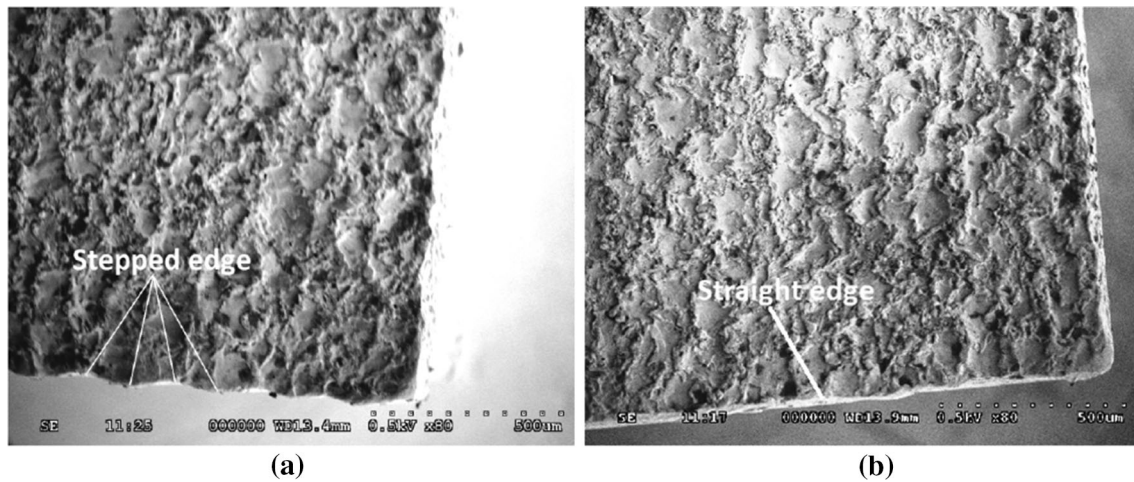


**Fig. 9** SEM micrographs ( $\times 80$ ) of machined surface/edge of Al/SiC<sub>p</sub>-MMC under two test conditions **a.** Run.6-  $T_{on} = 1.2 \mu s$   $T_{off} = 16 \mu s$   $SV = 30 V$   $I_p = 180A$   $WT = 850 g$   $WF = 8 m/min$  **b.** Run.29-  $T_{on} = 0.6 \mu s$   $T_{off} = 22 \mu s$   $SV = 30 V$   $I_p = 120A$   $WT = 1000 g$   $WF = 8 m/min$

for WEDM has been described in detail in various studies [29, 30]. In the present work, it is identified that wire vibration and deflection are the most important reasons of defect occurrences during machining of Al/SiC<sub>p</sub>-MMC which has not been yet investigated in detail. The study explores the effect of process parameters on the workpiece edge which is very important in terms of dimensional accuracy of final product. Figure 9a, b shows the SEM images of the machined edge generated under two experimental trials. By comparing at the same magnification, it is observed that higher pulse on time and lower wire tension generate step-like appearance on machined workpiece edge due to deflection or vibration of the brass wire during machining. It affects adversely the dimensional accuracy of the machined workpiece. The wire deflection is caused due to wire slackness at higher discharge energy and lower wire tension.

Figure 10 shows SEM of the machined surface having wire deflection marks (or band marks) when machining was carried out at run no.9 (i.e.,  $T_{on} = 0.9 \mu s$ ,  $T_{off} = 16 \mu s$ ,

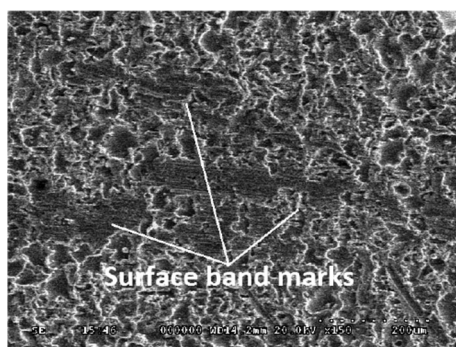


**Fig. 10** SEM micrograph ( $\times 150$ ) of machined surface band of Al/SiC<sub>p</sub>-MMC (Run.9- $T_{on} = 0.9 \mu s$   $T_{off} = 16 \mu s$   $SV = 20 V$   $I_p = 150A$   $WT = 850 g$   $WF = 8 m/min$ )

$SV = 20 V$ ,  $I_p = 150A$ ,  $WT = 850 g$ ,  $WF = 8 m/min$ ). It is believed that wire deflection marks on the machined surface are formed due to the erroneous feedback signal, which has been generated because of non-conductive dislodged SiC particles in the spark gap. This phenomenon might have occurred as the gap voltage sensor could not estimate the real gap in the presence of dislodged non-conducting SiC particles in the gap. The fast forward speed of wire may cause the wire electrode to collide with the workpiece material and form wire deflection mark on the machined surface. It is believed that the chances of occurrence of deflection mark can be reduced with the increase in wire tension. The influencing parameters such as spark gap voltage, wire tension and pulse off time need to be precisely controlled to minimize these surface defects. This phenomenon was also reported by Yan et al. [7], Patil and Brahmkar [10], and Habib and Okada [31]. Figure 5d shows the effects of spark gap voltage and peak current on SG. At the higher peak current, it can be observed that the SG increases sharply with parameter spark gap voltage. The increase, however, becomes gradual at lower peak current. It indicates a significant interaction between spark gap voltage and peak current. It could be observed that lower spark gap voltage and lower peak current combination results in lower SG.

From the ANOVA of spark gap shown in Table 4 and also from Fig. 5e, it is found that pulse on time is the major parameter affecting the SG (49%). The percentage contribution of wire tension, pulse off time, spark gap voltage and peak current on SG is 11%, 10%, 9% and 8%, respectively.

Analysis of the machined surface in terms of material diffusion between work material and wire electrode has been presented in the next section with the help of energy-dispersive X-rays (EDX).



### 6 Energy-dispersive X-rays (EDX) analysis

Complex chemical reactions among the work material, wire electrode material and the dielectric fluid are the basic elements of a WEDM process. The EDX spectra are taken to analyze the presence of elements on the machined surface of the workpiece. Figure 11a, b is the spectra when machining was carried out at high discharge energy and at low discharge energy, respectively. From Fig. 11a, it is clear that copper (3.25%) and zinc (3.75%) are present on the machined surface. However, the work material Al/SiC<sub>p</sub>-MMC has only 0.02% copper and does not contain any zinc element before machining. It clearly indicates that during machining these elements got diffused to the work material from wire electrode material. This may be due to the melting and re-solidification of the brass wire on the workpiece surface during machining. The specimen corresponding to run no.1 (i.e.,  $T_{on}=0.6 \mu s$ ,  $T_{off}=16 \mu s$ ,

$SV=30 V$ ,  $I_p=120A$ ,  $WT=1000 g$  and  $WF=8 m/min$ ) contains very less amount of copper and zinc into the machined surface as shown in Fig. 11b. From the figure, it is evident that at low discharge energy, the diffusion of wire constituents on the machined surface of the work material is low. The results are in agreement with the work of Goswami and Kumar [32]. The spectra of EDX also show the presence of carbon and oxygen. It is due to interaction of dielectric fluid which normally contains carbon and oxygen.

### 7 Conclusions

The wire electric discharge machining of Al/SiC<sub>p</sub>-MMC has been investigated based on Box-Behnken's design. The quadratic regression models have been developed to establish the relationships between the WEDM parameters and the selected responses (i.e., CS, SR and SG). The

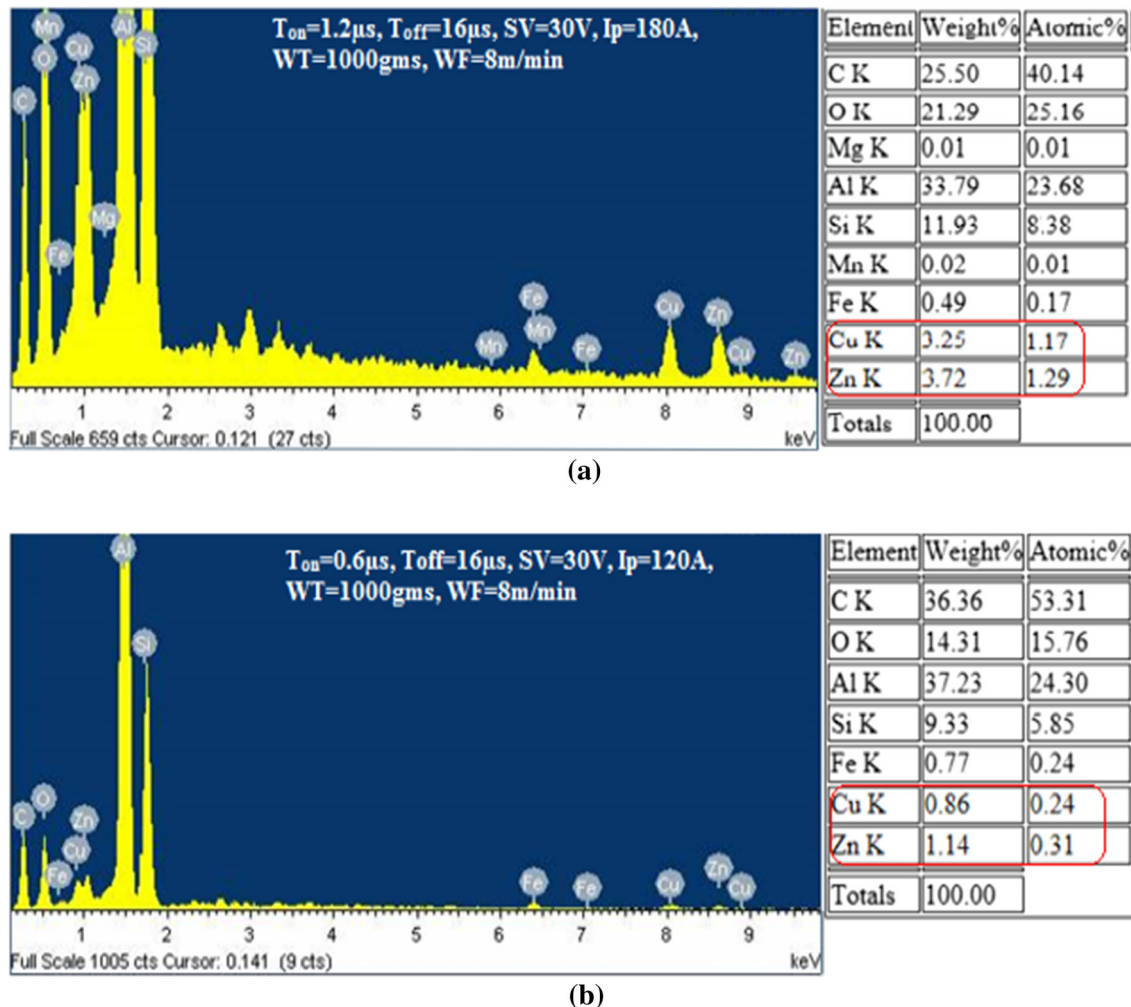


Fig. 11 Comparison of spectra of EDX of machined surfaces under two test conditions. **a** Run no. 6, Table 3 ( $T_{on}=1.2 \mu s$ ,  $T_{off}=16 \mu s$ ,  $SV=30 V$ ,  $I_p=180A$ ,  $WT=1000 g$ ,  $WF=8 m/min$ ), **b** Run no. 1,

Table 3 ( $T_{on}=0.6 \mu s$ ,  $T_{off}=16 \mu s$ ,  $SV=30 V$ ,  $I_p=120A$ ,  $WT=1000 g$ ,  $WF=8 m/min$ )

multi-response optimization results have been obtained using desirability function approach coupled with user's preference rating method. Based on the experimental results, the following conclusions are drawn:

1. Pulse on time has been found to be the most significant parameter affecting all selected response variables, while wire feed rate has little effect on responses.
2. The  $R^2$  values of the proposed cutting speed, the surface roughness ( $R_a$ ) and spark gap regression models have been found to be 0.94, 0.94 and 0.87, respectively, which signifies the ability of the models for making excellent predictions. Confirmatory tests also validate the same as maximum prediction error lies within 5.5%. The developed regression models will provide a guideline for the setting of WEDM parameters to get desired cutting speed, the surface roughness ( $R_a$ ) and spark gap.
3. User's preference rating method has been used to determine the weights for responses while desirability function approach has been used to combine the multiple responses into a single response. This optimization helps to determine the suitable process parameters for high cutting speed and low surface roughness,  $R_a$ , and spark gap.
4. The recommended process parameter setting for the WEDM process has been found to be the pulse on time = 0.7  $\mu$ s, pulse off time = 16  $\mu$ s, spark gap voltage = 35 V, peak current = 120A, wire tension = 1200 g and wire feed rate = 10 m/min in machining of Al/SiC<sub>p</sub>-MMC. It is the best parametric setting for an optimal performance taking into account the conflicting interests of multiple users.
5. EDX analysis of machined surface detected the basic elements of Al/SiC<sub>p</sub>-MMC workpiece and identified some residues such as Cu and Zn of the wire electrode material. The wire electrode material diffusion on the machined surface has been observed to increase with an increase in discharge energy.

Results thus attained through the exhaustive investigations in WEDM of Al/SiC<sub>p</sub>-MMC can serve as a useful reference to both the manufacturing engineers and the applied researchers in this field. This research work will open up the further scope to study the machined surface integrity and the underlying microstructural effects for utilizing WEDM in machining of Al/SiC<sub>p</sub>-MMC.

## References

1. Chawla N, Chawla KK (2006) Metal matrix composites, 1st edn. Springer, New York. <https://doi.org/10.1007/b101197>
2. Davim JP (2012) Machining of metal matrix composites. Springer. <https://doi.org/10.1007/978-0-85729-938-3>
3. Vedrtnam A, Kumar A (2017) Fabrication and wear characterization of silicon carbide and copper reinforced aluminium matrix composite. Mater Discov 9:16–22
4. Manna A, Bhattacharayya B (2003) A study on machinability of Al/SiC-MMC. J Mater Process Technol 140:711–716
5. Muller F, Monaghan J (2001) Non-conventional machining of particle reinforced metal matrix composite. J Mater Process Technol 118:278–285
6. Rao RV (2011) Advance modeling and optimization of manufacturing processes. Springer, Berlin. <https://doi.org/10.1007/978-0-85729-015-1>
7. Yan BH, Tsai HC, Huang FY, Lee LC (2004) Examination of wire electrical discharge machining of Al<sub>2</sub>O<sub>3</sub>p/6061Al composites. Int J Mach Tools Manuf 45(3):251–259
8. Tosun N, Cogun C (2003) An investigation on wire wear in WEDM. J Mater Process Technol 134(3):273–278
9. Patil NG, Brahmkar PK (2010) Determination of material removal rate in wire electro-discharge machining of metal matrix composites using dimensional analysis. Int J Adv Manuf Technol 51(5):599–610
10. Patil NG, Brahmkar PK (2010) Some studies into wire electro-discharge machining of alumina particulate-reinforced aluminum matrix composites. Int J Adv Manuf Technol 48:537–555
11. Shandilya P, Jain PK, Jain NK (2013) RSM and ANN modeling approaches for predicting average cutting speed during WEDM of SiCp/6061-Al MMC. Procedia Eng IConDM 64:767–774
12. Manna A, Bhattacharayya B (2005) Influence of machining parameters on the machinability of particulate reinforced Al/SiC-MMC. Int J Adv Manuf Technol 25:850–856
13. Patel K, Pandey PM, Rao PV (2008) Understanding the role of weight percentage and size of silicon carbide particulate reinforcement on electro-discharge machining of aluminum-based composites. Mater Manuf Processes 23(7):665–673
14. Shandilya P, Jain PK, Jain NK (2012) Parametric optimization during wire electric discharge machining using response surface methodology. Procedia Eng 38:2371–2377
15. Pramanik A (2015) Electrical discharge machining of MMCs reinforced with very small particles. Mater Manuf Process. <https://doi.org/10.1080/10426914.2015.1048360>
16. Das MK, Kumar K, Barman TK, Sahoo P (2014) Application of artificial bee colony algorithm for optimization of MRR and surface roughness in EDM of EN31 tool steel. Procedia Mater Sci ICMPC 6:741–751. <https://doi.org/10.1016/j.mspro.2014.07.090>
17. Mahapatra SS, Patnaik A (2007) Optimization of wire electric discharge parameters using Taguchi method. Int J Adv Manuf Technol 34:911–925
18. Fard RK, Afza RA, Teimouri R (2013) Experimental investigation, intelligent modeling and multi-characteristics optimization of dry WEDM process of Al-SiC metal matrix composite. J Manuf Process. <https://doi.org/10.1016/j.jmapro.2013.09.002>
19. Mahapatra SS, Patnaik A (2006) Parametric optimization of Wire EDM process using Taguchi method. J Braz Soc Mech Sci Eng 28(4):422–429
20. Garg SK, Manna A, Jain A (2016) Experimental investigation of spark gap and material removal rate of Al/ZrO<sub>2</sub>p-MMC machined with wire EDM. J Braz Soc Mech Sci Eng 38:481–491
21. Prasad DVSSSV, Krishna AG (2015) Empirical modeling and optimization of kerf width and wire wear ratio in wire electrical discharge machining. Int J Adv Manuf Technol 77:427–441
22. Assarzadeh S, Ghoreishi M (2013) A dual response surface-desirability approach to process modeling and optimization of Al<sub>2</sub>O<sub>3</sub> power-mixed electrical discharge machining (PMEDM) parameters. Int J Adv Manuf Technol 64:1459–1477. <https://doi.org/10.1007/s00170-012-4115-2>

23. Cheema MS, Dvivedi A, Sharma AK (2013) A hybrid approach to multi criteria optimization based on user's preference rating. *Proc Inst Mech Eng, Part B: J Eng Manuf.* <https://doi.org/10.1177/0954405413491958>
24. Montgomery DC (2001) *Design and analysis of experiments*, 5th edn. Wiley, New York
25. Kumar H, Manna A, Kumar R (2014) Analysis of parametric effects on response characteristics and faults diagnosis during WEDM of Al/SiC<sub>p</sub>-MMC. In: *Design and research conference (AIMTDR 2014) December 12<sup>th</sup>–14th, 2014, IIT Guwahati, Assam, India*, pp 702(1)–702(6)
26. Rao TB, Krishna AG (2014) Selection of optimal process parameters in WEDM while machining Al7075/SiC<sub>p</sub> metal matrix composites. *Int J Adv Manuf Technol* 73:299–314
27. Satishkumar D, Kanthababu M, Vajjiravelu V (2011) Investigation of wire electrical discharge machining characteristics of Al6063/SiC<sub>p</sub> composites. *Int J Adv Manuf Technol* 56:975–986. <https://doi.org/10.1007/s00170-011-3242-5>
28. Kumar A, Kumar V, Kumar J (2013) *Int J Adv Manuf Technol.* <https://doi.org/10.1007/s00170-013-4861-9>
29. Mouralova K, Kovar J, Klakurkova I, Bednar J, Benes L, Zahradnicek R (2018) Analysis of surface morphology and topography of pure aluminium machined using WEDM. *Measurement* 114:169–176
30. Arikatla SV, Manna KT, Krishnaiah A (2017) Parametric optimization in wire electrical discharge machining of titanium alloy using response surface methodology. *Mater Today Proc* 4:1434–1441
31. Habib S, Okada A (2016) Study on the movement of wire electrode during fine wire electrical discharge machining process. *J Mater Process Technol* 227:147–152
32. Goswami A, Kumar J (2014) Investigation of surface integrity, material removal rate and wire wear ratio for WEDM of Nimonic 80A alloy using GRA and Taguchi method. *Eng Sci Technol Int J* 17:173–184. <https://doi.org/10.1016/j.jestch.2014.05.002>